

## A Mini Review: Antireflective Coatings Processing Techniques, Applications and Future Perspective

Sadaf Bashir Khan<sup>1</sup>, Hui Wu<sup>1</sup>, Chunjiao Pan<sup>1</sup> and Zhengjun Zhang<sup>2\*</sup>

<sup>1</sup>The State Key Laboratory for New Ceramics & Fine Processing, School of Materials Science & Engineering, Tsinghua University, Beijing, 100084, China

<sup>2</sup>Advanced Key Laboratory for New Ceramics, School of Materials Science & Engineering, Tsinghua University, Beijing, 100084, China

\*For Correspondence: Zhengjun Zhang, Advanced Key Laboratory for New Ceramics, School of Materials Science & Engineering, Tsinghua University, Beijing, 100084, China, E-mail: zjzhang@tsinghua.edu.cn

Received date: Sep 01, 2017, Accepted date: Sep 18, 2017, Published date: Oct 09, 2017

Copyright: 2017 © Bashir Khan S, et al. This is an open-access article distributed under the terms of the Creative Commons Attribution License, which permits unrestricted use, distribution, and reproduction in any medium, provided the original author and source are credited.

### Review Article

#### ABSTRACT

Antireflective coatings (AR) are widely applied to eliminate the unwanted surface reflections from the AR coated substrate. In different optoelectronic devices, AR coatings have potential usage in photovoltaic solar cells, sensors, display devices, automobile industries to reduce reflectance, glare and enhance light transmittance. Natural phenomenon inspires researchers, and they generate bionic AR coatings copying the nature such as moth eyes, or cicada wings to fabricate efficient light harvesting AR coatings. In the current review article, we analyse and evaluate critically the progress and recent development in the fabrication of AR thin films comprising organic coatings, inorganic coatings, polymer AR coatings and bionic AR coatings. We predominantly emphasise the AR coatings fabrication by different methods and pinpoints the technological challenges in their real-world reliability. Finally, we address the future challenges and potential strategies for their upcoming prospect.

**Keywords:** Antireflective, Bionic coatings, Refractive index, Mechanical durability, Porous nanostructure

#### INTRODUCTION

The reflection is an optical phenomenon that is instinctive and proliferates due to light travelling in a medium having a different refractive index ( $n$ ) at interfaces. Light reflection is an undesirable phenomenon in various optical instruments such as eye wares, lenses, sensors but desirable in mirrors or filters. Researchers try to reduce this undesirable light by using different strategies, etching methods or patterning the surface with a film known as Antireflective (AR) coating to lessen the reflectance and enhance transmittance. The light reflected back at normal incidence angle is nearly 4% from a crown glass ( $n=1.52$ ) [1,2] and 36% from germanium ( $n=4.0$ ) [3] at the interfaces in air media at 550 nm wavelength. The reflected light influence and impede the optical element AR performance in two ways. Firstly, the reflected light lost from the main beam weakens the image. Secondly, a portion of reflected light when encroaches the image surface affects the contrast due to cloaking glare. Improvement in enhancing the light transmittance and reducing the reflective light in optical instruments has been achieved by using the appropriate AR coatings also known as "blooming". Fresnel equation endeavours the prefatory mathematical models of reflectance and reflection in optical elements during an interruption in light transmittance [4,5]. According to Augustin-Jean Fresnel, the incident light segment reflected back at the interface is measured as reflectance and transmittance measures shows the rest of light segment transmitted (refracted) [5]. The vector model to comprehend the light interference mechanism condition for a single AR coating is schematically presented in **Figure 1a**. The fundamental theory generating reflectance from AR layer depends on following presumptions, 1) the presence of homogeneous and non-absorbing medium between the incident light striking the optical surface and surrounding media, 2) optical scattering during interactions is considered negligible. Two conditions are necessary for achieving zero minima at a specific desired wavelength using a single homogeneous dense layer i) selecting the appropriate refractive index of coating material that lies midway between surrounding media and supporting substrate ii) the optical thickness of the AR coating is equivalent to one-quarter of the wavelength. When a

thin coating satisfy both the conditions, the reflection at the desired wavelength can be minimised nearly to zero. Mathematically, it is expressed as  $\eta_c = (\eta_o \eta_s)^{1/2}$  and  $d_c = \lambda / (4 \times \eta_c)$ . Here,  $\eta_s$  represents refractive index of the substrate,  $\eta_o$  is the refractive index of air,  $\eta_c$  represents refractive index of the film, and  $d_c$  is the thickness of the AR coating.

The key conceptions to lower the unwanted light at the interface of a substrate in air media is divided into three categories. The i) use of quarter wave AR coatings, ii) multilayer AR coatings or iii) graded index AR coatings to enhance light transmittance according to application demand.

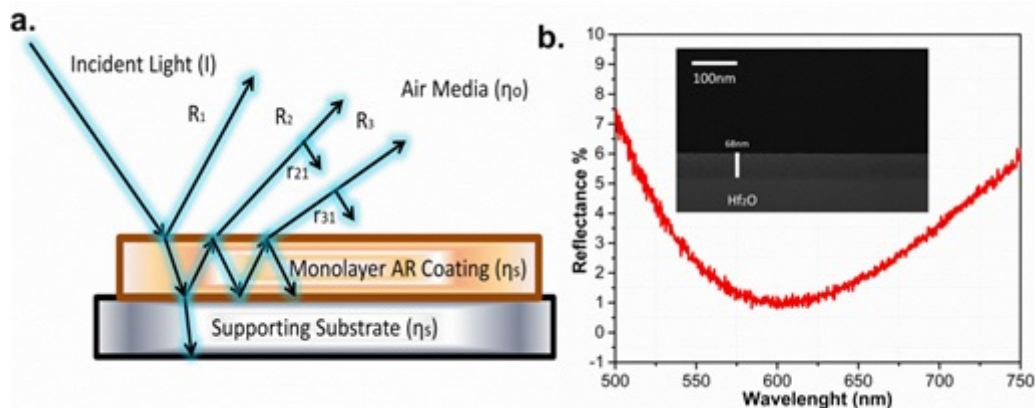


**Figure 1.** (a) Schematically representation of monolayer AR coating. (b) Represents AR efficiency of a single HfO<sub>2</sub> layer with SEM image in the inset.

Different methods have been proposed in fabricating transparent dielectric AR coatings comprises of single AR layer, multilayer AR coatings, or graded index coatings. AR coatings are applied and used either for aesthetic purposes or to enhance equipment functionality such as SiO<sub>2</sub> nanodomains on glass substrate increases transmittance up to 92% in comparison with uncoated glass (89%) applicable in photovoltaic applications by photolithography [6]. Layer by layer (LBL) deposition of mixed metal oxides gives 98% transmittance on quartz with super hydrophilic surface potentially apply to underwater imaging equipment. The water droplet of 2 ul spreads in <2 s on the mixed metal oxide coating [7]. HfO<sub>2</sub> AR coatings on silicon by magnetron sputtering shows the influence of annealing on AR due to increased  $\eta$  which increases the packing density of the thin film [8].

## SINGLE, BILAYER AND MULTILAYER AR COATINGS

The growing technological development in optics devices and optoelectronic equipment at industrial scale laid few demands on optical industry. The optical equipment at commercial level requires ultrathin coatings, AR proficiency at broader wavelength region and retaining AR efficiency at oblique light incidence angle beside the thermal resistivity and mechanical durability. Researchers used different scientific techniques to minimize undesirable light reflectance from the equipment surface. Different conventional approaches were used to lessen reflectances such as fabrication of single, bilayer or multilayers AR coatings. In photovoltaic industry, silicon is used as a primary absorbing material, a thin coating of an oxide having a thickness of 65 nm such as Si<sub>3</sub>N<sub>4</sub> ( $\eta=2.02$ ) reduces the reflection at 550 nm while remaining portion reflects nearly 5% reflection in the visible region [9]. Herein, we deposit dense HfO<sub>2</sub> ( $\eta=2.02$ ) monolayer film having a thickness of 68 nm on a silicon substrate using e-beam at a base pressure of  $3 \times 10^{-4}$  and deposition angle ( $\alpha$ ) is fixed at 0°. The ARM idea optics instrument is used to measure AR performance of as-deposited hafnia coating as shown in **Figure 1b**. We achieve a reflectance minima at 650 nm with a sharp increment of reflectance at both sides of wave minima in the visible region. The major disadvantage of monolayers AR coating is that it reduces reflectance at a specific wavelength and AR efficiency declines as the angle of light incidence (AOI) varies from normal incidence due to the difference in optical path length at oblique angles relative to a normal angle. Secondly, limited materials are available naturally having low  $\eta$  suitable for single layer AR coating requirement. The glass substrates ( $\eta=1.52$ ) required a single layer of coating having  $\eta=1.2$  which did not exist in nature. Usually, MgF<sub>2</sub> is used to deposit single layers on the glass because it has lowest  $\eta=1.32$  which exist naturally. Nowadays this issue is resolved by fabricating porous nanostructures by tuning the  $\eta$  of the coating through porosity [10]. Effective medium approximation calculations help in generating the fill factor and voids to create porous structures according to the desired requirements [11,12]. Polman and his colleagues use a sol gel and soft imprint technology method to deposit 120 nm monolayer SiO<sub>2</sub> nanocylinders having a diameter of 245 nm ( $\eta=1.20$ ) which diminishes reflectance to <0.57% in the visible region when monolayer porous silica coated on both sides of the glass [13]. The developmental progress in technological applications advances AR coatings and different monolayer nanostructured designs, composite patterned structures or polymer hybrids has been fabricated which possess low reflectance at broader spectrum region. The composite SiO<sub>2</sub>- Teflon coatings [14], SiO<sub>2</sub>/TiO<sub>2</sub> particles layer [15,16], TiO<sub>2</sub> AR coatings [16], SiO<sub>2</sub> polymer composite coatings [17], spirooxaize-polystyrene coatings [18], SiO<sub>2</sub> mesoporous

nanoparticles [19] or polymer AR coatings [20] are common examples of monolayer AR coatings which minimize reflectance at broader region without focusing on other properties such as mechanical thermal or non-wetting properties. Single layer AR coatings are applicable and desirable in different laser applications [21,22], photodiodes [23], light emitting diodes [24-26] or solar cell [27-31] applications. Due to the limited band width and reflectance minima at a smaller spectral region, these are not applicable to display devices, screens or eye wear optical equipment. The limitation of single dense layer coatings was restricted due to wavelength dependency, and nonfulfillment of omnidirectional AR performance.

The double layer AR coatings and multilayer coatings designs overcome this issue and fulfil the requirements. It has been experimentally proved that the  $\eta_e$  of bilayer AR coating decreases significantly at 500 nm when the  $\eta_e$  arrange in this order  $\eta_0 < \eta_2 < \eta_s < \eta_1$ . Bilayer coatings are known as v shape coating or w shape due to their reflectance curve [32,33]. The disadvantage of bilayer coating designs is that one cannot attain AR efficiency in a broad spectrum region. In double layer AR coatings usually, the top layer facing the surrounding medium (air) have lower refractive index than the bottom layer close to the substrate. To fulfil the destructive interference, the thickness of each layer in a bilayer coating is equivalent to half ( $\lambda/2$ ) or quarter ( $\lambda/4$ ) of the wavelength. Different research groups fabricate bilayer AR coatings following this principle, SiN and SiO<sub>2</sub> [34] deposited by Plasma Enhanced Chemical Vapour Deposition (PECVD) for solar cell applications, MgF/SiNx for crystalline solar cells [35], SiO<sub>2</sub>/TiO<sub>2</sub> self-cleaning AR coatings are few examples of bilayer coatings [36-38].

Xiao [39] fabricate a bilayer coating with tri wavelength AR performance using the sol-gel method. The thickness of the bottom layer was 113 nm ( $\eta=1.27$ ) prepared by acid catalysed and base catalysed silica sols. The thickness of the top layer was 245 nm ( $\eta=1.17$ ) developed by polypropylene modification of silica sols. Polypropylene not only induces hydrophobicity in AR films but also efficient in lowering the  $\eta$  of the top layer. They achieve reduced reflectance at 351 nm, 527 nm and 1053 nm wavelength with a light transmittance of 99.7%, 99.1.1% and 98%. One cannot neglect the hardness and non-wettability characteristics of AR coatings in case of exposure to the mild, humid environment for outdoor exposure. Majority of previous bilayer coatings focuses only on enhancing AR performance. It is a need to maintain a balance between the optical performance and the mechanical strength of AR coating before designing. Ruoyu Chen [40] fabricates bilayer composite coating by using silica and MgF<sub>2</sub> having  $\eta$  of 1.35 and 1.10 with an average light transmittance of 99.1% in the broader wavelength range covering visible and NIR region (400 nm-1400 nm). This coating possesses water contact angle of 152° after surface modification. The top layer is dense (porosity of 10.7%), so the bilayer coating passes the pencil hardness test (5H), and withstand against the critical load (Lc) of 27.05N. Composite coating of SiO<sub>2</sub> and TiO<sub>2</sub> shows omnidirectional AR efficiency and >99% transmittance on polycarbonate sheets and ophthalmic lenses [41]. Wavelength selective AR coatings by optimising the thickness and refractive index of the individual layer in a bilayer coating stack is also an advantageous factor in the optics field. Similar to single layer AR coatings, double layer coatings can also be prepared using a single material through tuning the  $\eta$  of coating material rather using composite materials which provide flexibility in designing double layer coatings. For example, SiO<sub>2</sub>, TiO<sub>2</sub> or HfO<sub>2</sub> were used in bilayer coatings on different substrates. We deposit a bilayer TiO<sub>2</sub> coating using e-beam at  $3 \times 10^{-4}$  base pressure on a silicon substrate using glancing angle deposition technique. We reduce the reflectance of silicon (36% at 550 nm) to <5% in a visible region with a wave dip at 550 nm and 650 nm applicable in different photovoltaics applications as shown in **Figure 2a and 2b**.

Xin-Xiang Zhang [42] design and fabricate a double-layer double-wavelength hydrophobic AR coating by template-free sol gel method which gives <1% reflectance at both 1064 nm and 532 nm for laser applications. They tune the  $\eta$  of the silica particles from 1.30 to 1.13 as shown in **Figure 2c**. The surface modification of bilayer coating considerably develops the hydrophobicity in bilayer film and increases the water contact angle from 23.4° to 160°. HfO<sub>2</sub> bilayer coating deposit by e-beam machine on quartz, FTO and crown glass give <1% omnidirectional AR performance with tunability in the visible wavelength range. These AR coatings are feasible for conductive optical instruments due to a dielectric characteristic of bilayer coating as shown in **Figure 3** [1,43,44].

Bilayer AR SiO<sub>2</sub> coating on a silicon substrate can reduce the reflectance (<0.01%) in the visible region for solar cell applications [45]. However, the limitation of this coating restricts their usage at broader scale due to top porous, fragile nature of coating which has weak mechanical strength. It is a future challenge to invent a mechanism to strengthen the porous AR layer for its usage in the optics field.

Multilayer coatings are similar to double layer AR coatings, comprises of alternatively high and low refractive index material to create destructive interference of reflected light. One can use a different combination of high and low refractive index dielectric films [46,47] single oxide film by tuning the  $\eta$  [43] or the mixture of dense or porous continuous layers depending upon the core application [47,48]. Multilayers AR coatings generate AR efficiency in the broader wavelength region or multi-dip in the desired wavelength range [49,50]. The SiO<sub>2</sub>, TiO<sub>2</sub> multilayer AR coatings are a most common combination of composite AR coating used as high and low index coating for achieving AR in a broader region on glass substrates [51,52]. There are various factors which limit usage of multilayer AR coatings, such as in the multilayer stack adhesion strength at interfaces, mismatch thermal properties of different oxide coatings, complex, intricate

fabrication process, mechanical stability decrement due to multilayer stacks, and expensive cost restricts their usage. Recently advancement in metamaterial AR coatings unlocks a new direction to fabricate ultra-thin coatings [53,54].

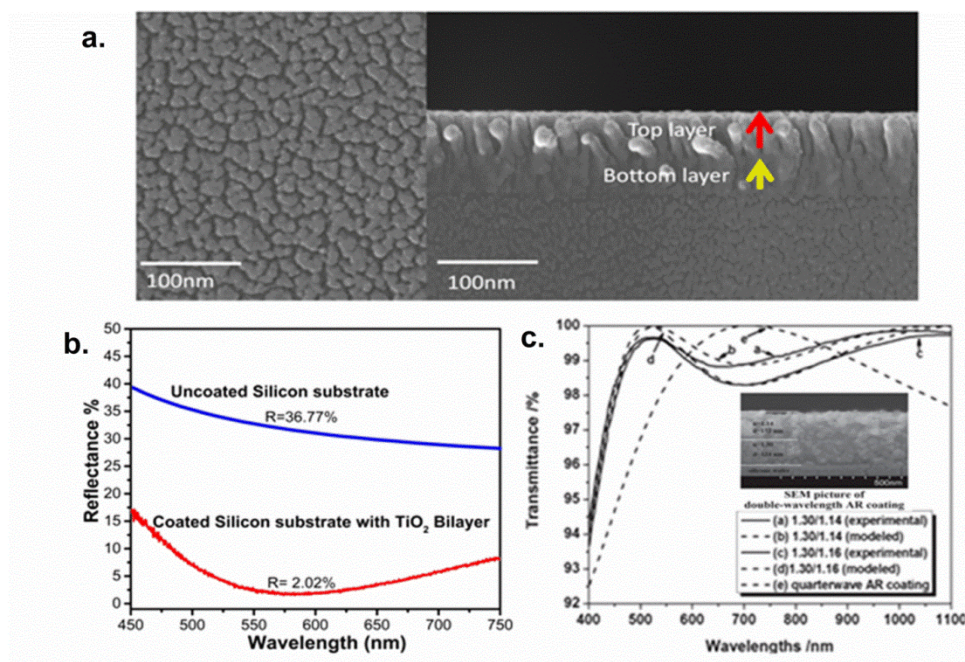


**Figure 2.** (a) represents SEM image of the top and cross sectional morphology of bilayer TiO<sub>2</sub> coating. (b) Reflectance measurement of TiO<sub>2</sub> bilayer coating on a silicon substrate. (c). Reproduced with permission [42] SEM image of double-layer double-wavelength broadband silica AR coating and Transmittance spectra of experimental and modelled double-wavelength AR coating.

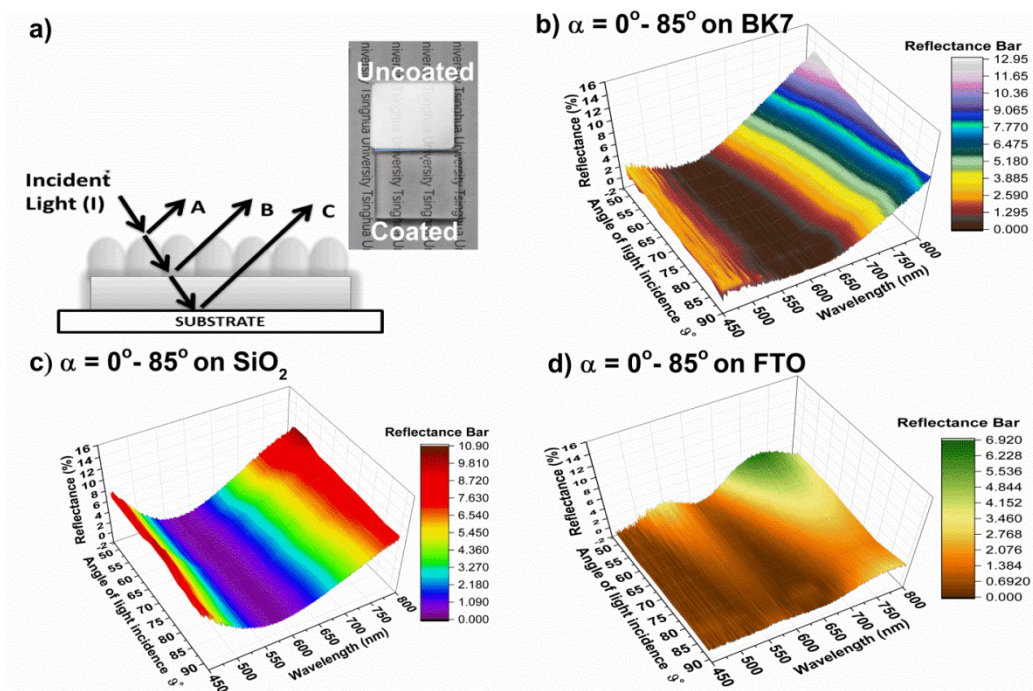


**Figure 3.** Reproduced with Permission [44] (a) Schematic representation of a designed bilayer AR coating. The inset shows the AR efficiency comparison of coated and uncoated glass (BK7). Omnidirectional reflectance results of bilayer HfO<sub>2</sub> AR film on (b) BK7 (c) SiO<sub>2</sub>, and (d) FTO.

## FABRICATION METHODS

Different fabrication method and techniques have been used for the preparation of AR thin films. The approach of fabricating AR films splits into two broad categories i-Bottom up and ii-Top down approach. The bottom up fabrication includes methods such as sol-gel processing [55-58], chemical vapour deposition (CVD) techniques [59-61], magnetron

sputtering [52,62], plasma-enhanced chemical vapour deposition [63-65] or physical vapour deposition (PVD) techniques [66,67]. The top down approach is limited to wet and dry etching methods. Much research has done on AR coatings by using PVD or CVD methods to generate excellent omnidirectional AR coatings for practical purposes. Herein we review few techniques in brief and the coating AR efficiency.

### Bottom Up Approaches

**Sol-gel techniques:** In sol-gel method high chemically active ingredients mixed in liquid form which was used as a precursor. Different metal organic precursors such as alkoxides, carboxylates, diketones or organic salts are used to initiate reactions. A transparent sol films form as a result of condensation reaction or hydrolysis. Later the sol polymerises into a gel which is a 3D-structure of the continuous solid network with no flowing fluid. Lastly, the nanostructure sol-gel derived film form by curing. The sintering and drying steps performed according to one's required condition. The major advantage of sol gel technique in fabricating thin films is that one can easily alter the surface chemistry and control the refractive index of thin films through precursors. Different parameters influence the final sol gel prepared AR coatings such as chemical mixings, concentration, temperature, component ratio, substrate material, fabrication technique or sequence of mixing. Sol gel technique is sub divided into different categories including dip method [68], a spin method, and laminar flow method. The sol-gel processing technique is widely used in silicon solar cell applications. Various organic-inorganic metal oxides coatings were fabricated by using sol gel technique such as  $\text{HfO}_2$  films [69].

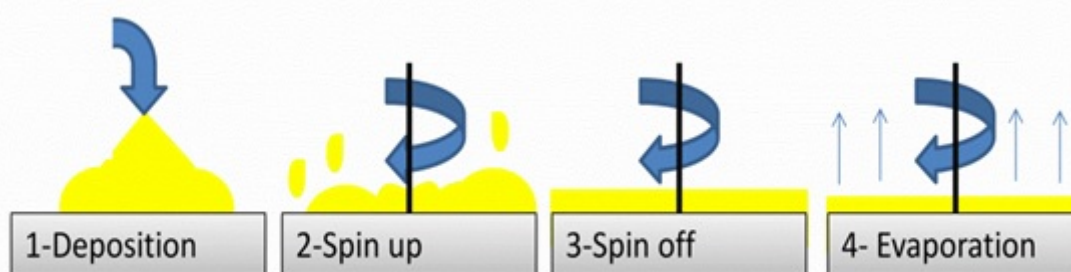


**Figure 4.** A graphic demonstration of the spin coating method.

**Spin coating:** The spin-coating technique is broadly employed to organic, inorganic, organic-inorganic solution mixtures for fabrication of thin film coatings over large areas with structural uniformity. In the spin coating method; the substrate rotates around an axis which is perpendicular to coating wafer. The coating thickness controlled by spin speed, solution viscosity and spin time [70]. Four steps are involved in spin coating fabrication which involves deposition, spin up, spin off and evaporation as shown in **Figure 4**. In the first step, to avoid discontinuities in film preparation large amount of liquid is deposited on a spinning substrate which rotates slowly. In spin up process the substrate wafer is rotated at high speed for the formation of uniform, homogeneous film by generating wavefronts which flow towards wafer edge. The spin off stage is the process where an excess amount of deposited solvent is removed by rotating the wafer between 2000 rpm to 8000 rpm, and the fluid is thin to a level where its flow ceases and viscosity increases. Evaporation is the last and final step, on which thin film properties are dependent. If evaporation step is carried out before thin film generation, then it generates certain defects in the coatings. Various variety of densely ordered thin films formation takes place by controlling spinning speed [71]. Kikuo Okuyama, et al. [72] fabricate monolayers  $\text{SiO}_2$  on a sapphire substrate having 300 nm particle size with average surface coverage of 72%, and transmittance of >80% in the visible region, in a time interval of 25 seconds. Similarly, Ganguli fabricate  $\text{SiO}_2$  coatings with a particle size of 34 nm on a borosilicate crown glass substrate by spin coating reducing reflection <4% in the NIR range (900 nm–1250 nm) [73] having a refractive index of 1.21 and a porosity of 68%. Much research has been done on  $\text{SiO}_2$  nanoparticles and thin film fabrication for omnidirectional light harvesting AR coatings to its potential applications in solar cells at commercial level using the spin method [31,74-78].

In comparison with organic and inorganic materials, polymer materials also show a huge tendency in the optics field. Due to availability, easy processing and strong adherence to supporting substrates, especially strong adhesion to plastic substrates makes it applicable to commercial use. Earlier different approaches for manufacturing porous polymer films have been suggested which achieve ideal AR efficiency. Zhang et al. [79] have demonstrated to fabricate PAA/PDDA-silicate multilayer films in the visible wavelength region with a light transmittance of 99.86% on a quartz substrate by a layer-by-layer (LBL) technique. However, few AR coatings had limitations and restricted to the spectral range of certain wavelength and the effect of light incidence angle influences the transmittance properties [80-82].

Han, et al. [7] established an efficient technique for preparing polymer AR films with gradient refractive index. They obtained a polystyrene-block-poly(methyl methacrylate) (PS-b-PMMA)/onto an octadecyl trichlorosilane (OTS)-fabricated on both sides of the glass as supporting substrate using the spin-coating at 3500 rpm for 30 s. They obtained a porous nanostructure with gradient porosity in the vertical direction. They fabricate four different nanocoatings by changing concentration (18, 27, 32, and 36 mg mL<sup>-1</sup>) using tetrahydrofuran and toluene to control the gradient porosity ratio and film thickness which increases from top to bottom of the coating. The AR film having a thickness of 27 mgL<sup>-1</sup> shows better AR performance in visible and NIR region in comparison with other porous AR coatings using different concentrations such as 18 mgL<sup>-1</sup> (71 nm) are thin enough to satisfy AR performance. The 32 mgL<sup>-1</sup> (287 nm) thickness shows declination in transmittance as represented in **Figure 5**. The prepared polymer graded film having a thickness of 225 nm gives broadband omnidirectional AR (97%) in the visible (400 nm-800 nm) and (800 nm-1200 nm) NIR light range [55] for a different angle of incidence (AOI) between 0° to 60° (**Figure 1b**).

The advantage of their fabrication technique is that it did not require any post-treatment or multiple steps, i.e. annealing temperature. The main disadvantage of spin coated AR coatings is that it is hard to fabricate AR coatings on commercial scale applications as the large substrates cannot be used and spun at a necessarily high rate.

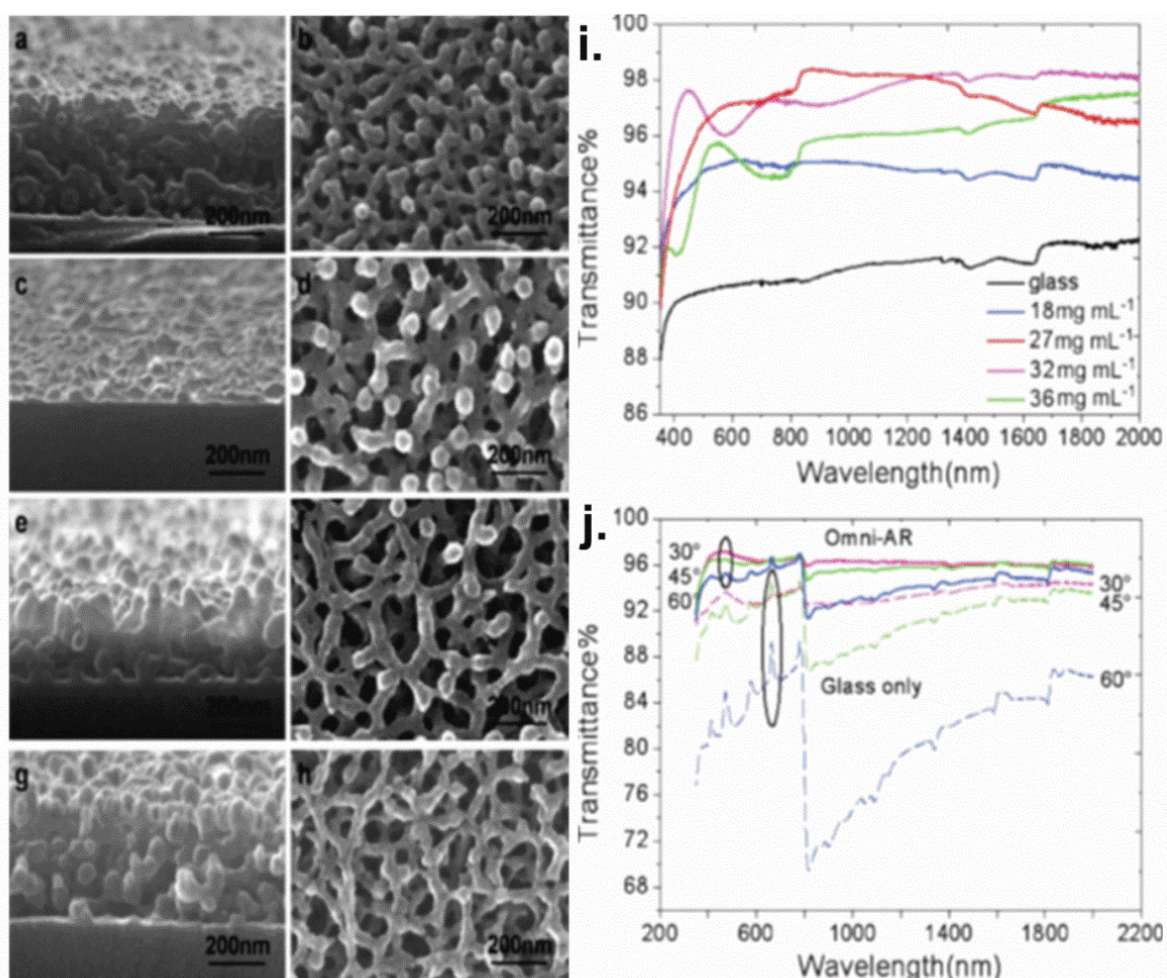


**Figure 5.** Reproduced with permission [55]. SEM images of nanoporous AR Films with different solution concentrations: (a,b) at 27 mg mL<sup>-1</sup> (c,d) 18 mg mL<sup>-1</sup>, (e,f) 27 mg mL<sup>-1</sup>, (g,h) 36 mg mL<sup>-1</sup>. (i) Transmission spectra of porous films on the glass substrates at normal incidence. (j) The transmittance of the glass at various AOI before and after the porous films coating.

**Dip coating:** In dip coating, the colloids are evaporation induced and self-assembled on the wafer substrate as it slowly withdrawn from the colloidal suspension. **Figure 6** schematically represents a supporting substrate immersed in required sol to form a wet thin layer. According to experimental requirements, the substrate is withdrawn from the liquid under control temperature and atmospheric conditions. The surrounding atmosphere controls the evaporation of solvent which leads to gelation in the result of film formation [83,84].

Thermal treatment then densifies the film, and densification temperature depends on compositional constituents of the fabricated coating. Cathro [85] device a procedure of fabricating SiO<sub>2</sub> AR coatings using ethanol based silica sol to

enhance the transmittance, on the cover plates of the collector using dip coating method to eliminate 60 percent of reflectance losses. Vanadium oxide coatings prepared by dip coating enhance light transmittance after lyophilization [86].

TiO<sub>2</sub> nanotexture [87] coatings used as cover cells prepared by dip coating (6mm/sec) gives optical transmittance with self-cleaning ability applicable in PV cells. The major disadvantage of this technique includes the slow fabrication process, in comparison with other methods. Secondly, the small coating area, the non-uniformity of the final product, or the usage of chemicals are often too reactive to corrode the substrate itself.

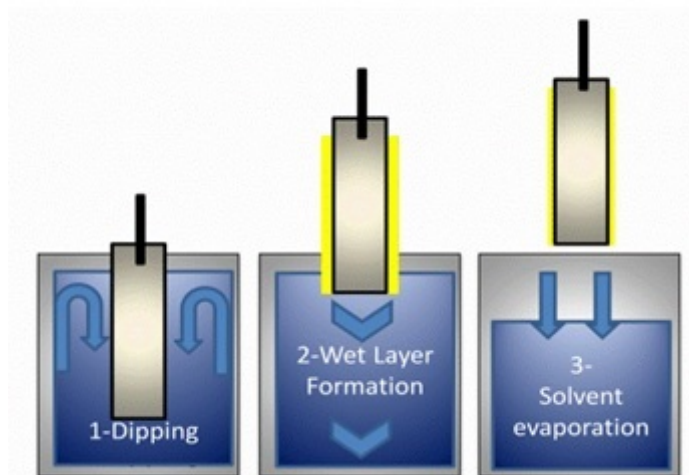


Figure 6. A graphical illustration of the dip coating technique.

### Physical Vapour Deposition (PVD)

Physical vapour deposition technique refers to vacuum deposition method which comprises of three steps including vaporization of the target material, transferring from target towards substrate and deposition on the substrate. The most common PVD methods are electron beam physical vapour deposition [88,89], sputter deposition [2,90], pulsed laser deposition [91,92] and cathodic arc deposition in which the material undergoes from a condensed phase to a vapour phase for the formation of thin films or coatings. PVD method plays an influential role in controlling the morphology, thickness and porosity of deposited thin films. Earlier productive research has been done on AR coatings fabrication practically applicable in optics field and eye wear equipment [93].

Magnetron sputtering is used to deposit, AR coatings on large flat substrates including TV screens and computer monitors [94]. Bartzsch, et al. [95] fabricate rugate filters which give <0.5% reflectance in 440 nm to 620 nm wavelength region. These narrow band rugate filters have potential applications in laser applications and protective goggles. Colour AR coatings fabricated by magnetron sputtering have potential application in architecture and cement industry [96]. One can easily generate highly porous and different nanostructures by optimizing fabricating parameters. Oblique angle can easily change the density of films in comparison with dense film. Similarly, SiO<sub>2</sub>  $\eta$  reduces from 1.45 to 1.05 and TiO<sub>2</sub>  $\eta$  from 2.54 to 1.30 by changing the deposition angle [97,98]. The oblique angle deposition helps in fabricating AR coatings to reduce reflectance at broader wavelength range [99]. Previously different research groups focus on depositing multilayer composite AR coatings using TiO<sub>2</sub>-SiO<sub>2</sub> as a target material to induce a gradual change in  $\eta$  and control the porosity in thin films [100]. HfO<sub>2</sub> films [69] on FTO and sapphire substrate also shows broadband AR efficiency in the visible region.

Glancing angle deposition technique (GLAD): GLAD technique plays an influential role in controlling the porosity by nanotexturing the coating material. This technique not only controls the porosity of individual layer but also induces a gradual change in refractive index from top to bottom substrate in surrounding media. One can deposit different nanostructures with varying porosity and mass flux in a coating by controlling fabricating parameters including glancing angle, substrate static state or rotational condition, deposition rate, base pressure and deposition time duration according to experimental need [101-103].

Zhang, et al. [42] change the HfO<sub>2</sub> refractive index from 1.9 to 1.30 by varying the oblique angle ( $\alpha$ ) from 0° to 88° at a 550 nm wavelength as shown in SEM image of monolayer HfO<sub>2</sub> deposit at various glancing angles in Figure 7 [1,44]. Oblique angle highly influences the nanostructure morphology due to self-shadowing effect. One can tune the ratio of voids and mass flux by glancing angle. The nanocolumns become more oriented and highly uniform, with the distinguishable structure formation by varying  $\alpha$  in comparison with lower glancing angles.

Figure 7 shows the transformation of bulk thick film to highly porous film under the influence of deposition angle. The  $\eta$  of monolayer HfO<sub>2</sub> measured at 550 nm wavelength shows declination with increasing  $\alpha$  due to the formation of voids

and pores in as-deposited films. The Glad technique is significant in modifying nanostructure of monolayer or multilayer coatings by controlling  $\alpha$  and fabricating parameters.

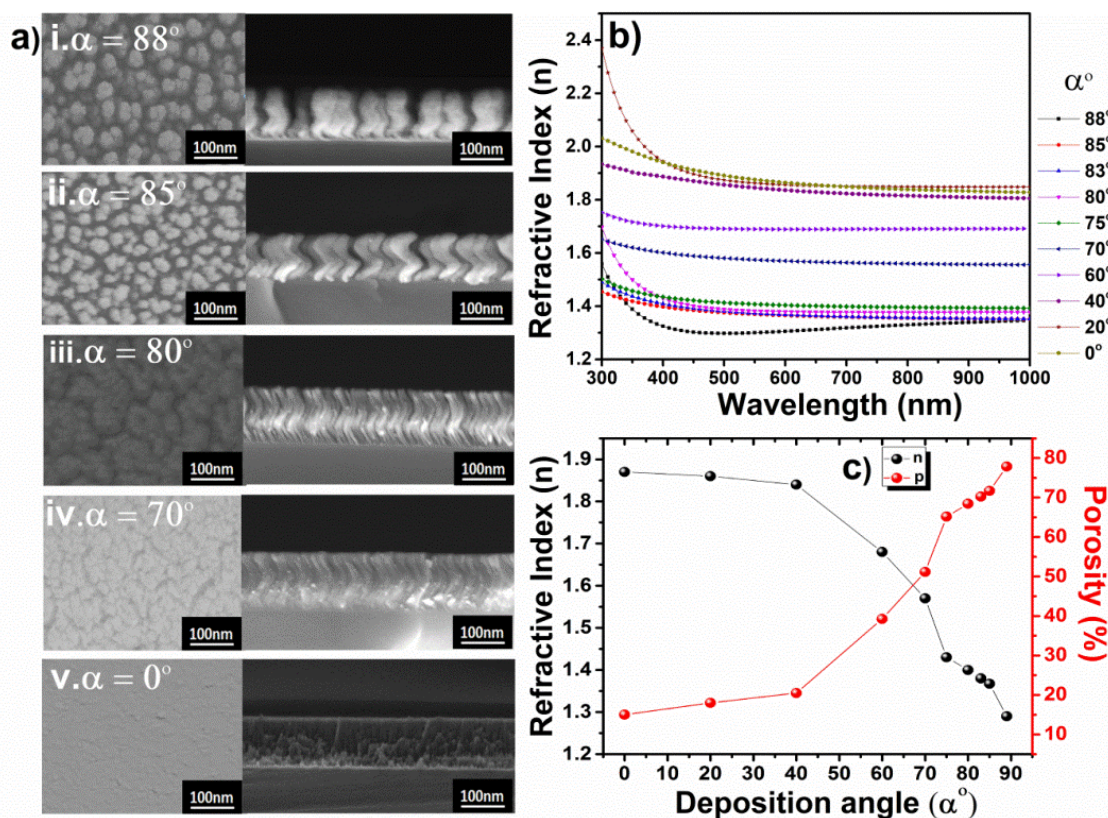


**Figure 7.** (a) Reproduced with permission [1]. Top and cross-sectional SEM images of the single-layer HfO<sub>2</sub> film deposited at various glancing angles ( $\alpha$ ). (b) Refractive index of mono layer hafnia films as a function of wavelength. (c) refractive index  $\eta$  at 550 nm wavelength and the calculated porosity as a function of deposition angle  $\alpha$ .

SiO<sub>2</sub> and TiO<sub>2</sub> graded index film in which the progressive change in  $\eta$  is carried out by changing the density of pores and fill factor ratio of air with in the individual layer using magnetron sputtering [104]. Up to that time, considerable exploration is done on fabricating AR coatings using the GLAD technique.

Chhajed [105] fabricate SiO<sub>2</sub> AR coatings and tune the  $\eta$  from 1.47 to 1.07 by varying deposition flux through oblique angle deposition and reduces the reflectivity of silicon from 37% to 5.05% in visible and NIR region (400 nm-1100 nm). Similarly, Zhang group [43] establish a simple method to fabricate broadband AR coatings using Glad technique with a single material Hafnia on sapphire and FTO using the GLAD method. They change the refractive index of the individual layer in a trilayer coating by changing the deposition angle in a single step to avoid impurity or dirt particles. The oblique angles for deposition were 0°, 80°, and 88° for trilayer graded refractive index coating. The deposited films show omnidirectional AR with thermal stability up to 300°C suitable for the thermal operative equipment.

Nowadays different groups are trying to deposit polymer coatings using e-beam. Our group is also one of the pioneers in depositing polymer AR coatings using the GLAD technique. We deposit Teflon on FTO (Fluorine doped tin oxide) substrate at  $\alpha=86^\circ$  on one side of the substrate and reduces its reflectance from 9% in the whole visible region to nearly 1% through Teflon coating as shown in **Figure 8**.

The fabricated coating gives omnidirectional AR efficiency applicable to conductive optoelectronic instruments. The benefit of Teflon AR coatings is that they possess self-cleaning ability without any post surface treatment due to fluoropolymer presence which makes them oil repellent and water repellent. The chief reason which restricts their usage in real applications is the intrinsic fragile nature of the top nanoporous surface structure. However, the upper porous geometrical structure and surface modification contribute positively to self-cleaning ability in an exposed humid environment.



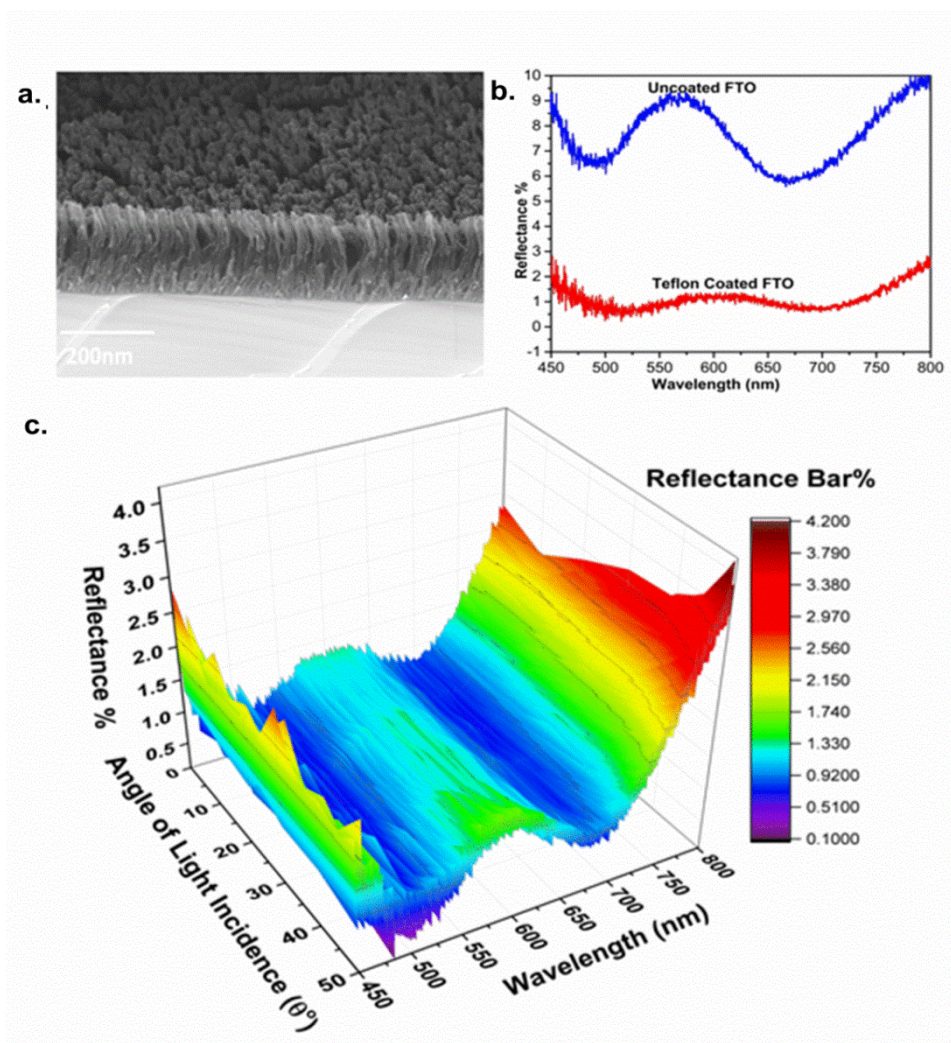


**Figure 8.** The SEM image of Teflon AR coating deposited on FTO by GLAD technique. (b) Measured reflectance at normal incidence of Teflon coated and uncoated FTO. (c) Omnidirectional AR performance of Teflon coating.

### Top Down Approaches

**Etched coatings:** Fraunhofer was the first one who notices that etched glass minimizes the reflectance and discovers it accidentally, that the reflection decreases when the coating surface is etched with sulphur and nitric vapour atmospheric exposure. A biomimetic replication method was based on this concept. Jiang and his colleagues used this simple concept of etching to reduce the surface reflectance  $<1\%$  in visible spectrum [106]. Similarly, Wl.Min group reports the fabrication of moth-eye nipple nanoarrays on gallium antimonide substrates using etching method. Their coating exhibits broadband anti-reflectance applicable for thermovoltaic applications [107]. Ho Won Jang [108] develops an economically low-cost method to fabricate hierarchically nanotextured glass with silica beads using dry etching to generate super hydrophobic self-cleaning AR coatings with water contact angle of  $158^\circ$  and reflectivity of  $<4\%$  in the visible spectrum. Lifeng Chi [109] group develop silicon nanocones on a silicon wafer to generate high-performance AR coatings with  $0.7\%$  reflectance in the broader wavelength range of 400 nm 1050 nm exhibiting super-hydrophobic property ( $164^\circ$ ) after fluorination. Etching silicon surface under different conditions opens a gateway in solar applications at commercial scale. Pyramidal nanostructures fabricated by etching silicon wafer is very useful in AR coating applications [110]. The geometry, i.e. cylinders, pyramids, square shape, size, the diameter of nanostructures and height of nanostructures greatly influence the final AR performance of the coating. The nanotexture behaves as a gradient index film based on effective medium approximation and fill factor. A different process is developed for AR coatings for solar cell applications such as electrochemical etching of silicon solar cells [111]. Similarly, Porous silicon was fabricated on multi-crystalline Si substrates using stain etching in aqueous HF/HNO<sub>3</sub> solutions. Fabricated porous Si structure reduces surface reflectance  $>3\%$  in a wavelength range (400–800 nm) [112]. One can modify and tune the refractive index of pores diameter and pitch in SiO<sub>2</sub> by using hydrofluoric acid [113]. Chemical and electrochemical etching is used to fabricate AR coatings for silicon solar cell applications, but the major drawback which limits this approach is the brittle nature of porous layer [113]. Numerous research groups also focus on polymer AR coating through chemical etching. Chemical

etching method to generate AR coatings were commonly used in the 20<sup>th</sup> century due to the easy fabrication process and low-cost [114,115]. In chemical etching, the etchant dissolves leachable components to produce a porous AR coating having lower  $\eta$  than the substrate material. The major drawback of chemical methods is that they require a significant amount of surfactants, or sometimes chemicals are too reactive that they corrode the substrate itself, or sometimes by-product formation influences the AR efficiency of the final coating or accumulation of impurity or dirt during processing also influences the AR performance.

### Bionic AR Coatings

Bioinspired AR coatings such as Moth eyes also known as compound eyes are used in generating efficient AR coatings. Bernard was the first researcher who studies the outer corneal lens surface of moth eye and deduces the height of conical protuberances is nearly 200 nm [107]. Later on, moth eye structure was further investigated by Clapham and Hutley followed by different research groups [116]. Moth eye nanostructure on glass enhances transmittance to 99.80%, but these coatings are practically not applicable due to the fragile structure. The corneal nipples are highly order oriented and uniformly arranged [116]. Different research groups fabricate AR coatings replicating moth eyes nanostructure such as JW Leem group [117] prepare moth eye conical nanopatterned films on the glass surface by soft imprint lithography technique. The fabricated films are hydrophobic with a water contact angle of 112° and transmittance of 93% in the broad spectral range covering the visible and NIR region (350 nm-1800 nm). The coatings show excellent thermal stability under UV exposure (10 hours), and heat treatment of 120°C. These coatings have potential applications in GaInP/GaInA PV modules as it enhances the current density from 14.68 to 14.07 at normal light incidence angle. Besides this, it also shows omnidirectional AR efficiency over wide range of light incidence angle from 10°-70°. This moth eye patterned nanostructures possess wide angle AR efficiency with hybrid properties beneficial in multijunction photovoltaic applications [117]. Similarly, moth eyes like nanopillars on the convex lens were fabricated by self-assembling nanoparticles and plasma etching the lens enhance light transmittance due to the gradual change of refractive index from surrounding air media and <1% reflectance at 590 nm wavelength region. Such coatings are applicable on camera lenses to reduce glare and glaze images due to the total internal phenomenon. Moreover, surface modification with fluorinated polymer enhances its hydrophobic and self-cleaning ability without influencing its AR efficiency [118].

## APPLICATIONS

One cannot deny AR coating impact, use and significance in today's high-tech evolving technology from industrial application towards medical and bioengineering field. Emerging technology and businesses demand increases interest to innovate multifunctional AR coatings. On a commercial scale, AR coatings have been employed as an integral segment to increase the output efficiency of different electro-optical devices. AR coating is an essential component in solar cells, light emitting diodes (LEDs), telescopes, flexible display devices, ophthalmic, cathode ray tubes (CRTs) [119], liquid crystal display devices (LCDs) [120] display panels, outdoor panels [121], or in automobile industries to enhance light transmittance [122]. The fabrication process, substrate selection, material choice, refractive index, precise thickness and uniformity of AR coating are crucial to accomplish high performance and good yield in optical devices. AR coatings on LEDs enhance the output power by low power consumption and reduce the device heating due to entrapped photons inside the chips. H.K. Lee deposit Sb/SnO<sub>2</sub> on AlGaInP and improves the output power to 26% at 350 mA without deteriorating the electrical performance in comparison with conventional LED [119]. T Kondo enhances the efficiency of nitride LEDs on sapphire and SiC substrate up to 3.7% and 3.2% by surface texturing and replicating moth eyes using low-energy electron-beam projection lithography (LEEPL) [123]. Yan, et al. [124] deposit omnidirectional bilayer alumina AR coating on sapphire and improve the light extraction efficiency up to 8% for LEDs required in deep-UV photosensitive devices. The deep-UV optical devices are needed in flame monitoring, optical fibres, interferometric lithography, detectors lenses or femtosecond lasers [125]. Earlier, various research groups remarkably improves the LED efficiency using AR coatings such as UV-LED of GaN doubles the efficiency at 365 nm wavelength [126], Al<sub>2</sub>O<sub>3</sub>-InP/InGaAsP LEDs for optical communications [127], LEDs-optical lenses [128] Al<sub>2</sub>O<sub>3</sub>-TiO<sub>2</sub> AR coating for red light organic electroluminescent devices [129], Al nanoparticles by co-sputtering for GaN-LEDs [130-132] Al<sub>2</sub>O<sub>3</sub>-ZnO<sub>2</sub> GaN-LEDs [133-136], ZnO<sub>2</sub>-LEDs [132,135], Indium tin Oxide nanorods for LEDs [137-140]. Some of these methods are applicable commercially, but few of them are restricted to labs due to costly groundwork, difficult process and damaged induced procedure while few techniques limited to small area LEDs with minor current values. It is a prerequisite to progress a cost effective AR fabrication method with reliable product and standard quality.

Similarly, AR coatings on Photovoltaic devices remarkably boosts up the instrument performance. Natural resource usage such as solar energy is an environmentally friendly renewable energy source in Photovoltaic (PV) devices to enhance power conversion efficiency. In commercial photovoltaic modules, solar glass is an integral component to protect the solar thermal collectors from atmospheric; climatic changes and harsh environmental conditions. In solar modules, the front exposed glass surface without an AR coating reflects nearly 4% sunlight and decreases the overall

efficiency of solar cells<sup>[141]</sup>. The AR coating in photovoltaic applications enhances the solar cell efficiency and minimize the reflection losses. The AR coatings on glass cover play a vital role in PV devices protection from weathering and climatic exposure. Different research groups established advanced methods for fabricating AR coatings to enhance the solar cell operational efficiency<sup>[141,142]</sup>. The soda lime glass, float glass, borosilicate glass or cast glass is commonly used in PV optical devices<sup>[142]</sup>. San Vicente<sup>[141]</sup> fabricates silica AR coatings on borosilicate glasses using sol-gel method achieving stable (0.97%) transmittance and long-term durability (>1 year). Paula, et al.<sup>[143]</sup> examine and study the silicon PV degradation mechanism after its environmental exposure for long duration using different techniques of visual inspection, electrical conductivity evaluation and infrared thermography. They conclude that delamination, abrasion, AR coating oxidation, corrosiveness and glass weathering were major defects which influence the PV efficiency. Different factors influence the final efficiency of PV modules including installation site, mounting conditions, and manufacture process. Jia Li<sup>[144]</sup> reports TiO<sub>2</sub>/SiO<sub>2</sub> and ZrO<sub>2</sub>/SiO<sub>2</sub> bilayer AR coatings on PV modules and compare its mechanical durability with porous SiO<sub>2</sub> layer showing increased mechanical durability and thermal resistivity up to 121°C temperature. Ultraviolet (UV), AR coatings fabrication by using polysilanes as a bottom AR layer for KrF (248 nm) laser, is used to enhance durability<sup>[145]</sup>. Incorporation of carbon nanotubes and graphene based PV silicon heterojunction modules open a new trend to improve PV modules productivity<sup>[146]</sup>. Fen Lu, et al.<sup>[146]</sup> enhance polymer solar cell efficiency up to 16% using single wall carbon nanotubes (SWNT-0.125% weight) which provide an efficient pathway for charge transfer. Previously much commendable research is done to enhance solar cell efficiency. SWNT/quantum dot sensitized solar cells (QDSSCs)<sup>[147]</sup>, Polymer PV with Ag-ink jet<sup>[148]</sup>, PbSe incorporation in solar cells<sup>[149,150]</sup>, functional SWNT for improving PV yield<sup>[151,152]</sup> or polyaniline nanotubes assimilated in polymer solar cells<sup>[153]</sup>. Few of them are not applicable to real life applications on large scales production due to thwarting fabrication process. The PV modules require AR coatings to entail specific standards including broadband wavelength, stable AR performance according to PV modules lifespan (>20 years) and low fabrication cost<sup>[154]</sup>. The International Electrochemical Commission (IEC) provides a standard module test according to which the solar module have to tolerate the heat trial for nearly 1000 hours<sup>[154]</sup>.

Besides this, AR coating also improves the visual performance of display devices, cameras, lenses, eye wear or LCDs such as multilayer coating (Sb-SnO<sub>2</sub>-TiO<sub>2</sub> SiO<sub>2</sub>) on CRT tube enhance the AR performance of CRT<sup>[155]</sup>. In LCDs combination of altering metal (10 nm-40 nm) and nonmetal (<40 nm) thin layers increase the brightness<sup>[120]</sup>. TiO<sub>2</sub>-SiO<sub>2</sub> composite AR coating fabrication by magnetron sputtering<sup>[52]</sup>, multilayer AR coatings for display panels or monitors<sup>[156]</sup>, AR coatings on display filters<sup>[157]</sup> have high light transmittance, and it also provides electromagnetic interference shielding. AR coatings on plasma display panels<sup>[158,159]</sup> or SiO<sub>2</sub> AR coating by dip method for screens system in aeronautic and aviation field<sup>[160]</sup> improves the instrumental performance significantly. The practical exposure of AR coatings in any technology either PV applications, display devices, LEDs, or any optical instrument, AR durability, adhesion strength and anti-corrosion properties are of vital importance to ensure its consistent performance and reliability which requires additional detail investigations.

## CONCLUSION AND FUTURE PERSPECTIVE

One cannot repudiate the importance of AR coatings in today's routine life as briefly discussed in outline and AR applications. The AR coatings are used in broad range of emerging applications in optics fields including different industrial fields, from submarines, military equipment, solar cells, light emitting diodes, glasses, laser applications, aeronautical sensors, or automotive, industrial applications including optoelectronic devices etc.<sup>[161]</sup>. Nowadays fabricating hybrid coating is very common for low emissive applications with self-cleaning AR ability. The integration of AR property together with electrochromism opens a new way of technological development. One such example is titania-based tungsten AR composite coatings with photo electrochromic efficiency<sup>[162]</sup>. The research on thermochromic AR coatings also open another direction, in optoelectronics field such as VO<sub>2</sub> thin film smart coatings can be used in space craft sun shields, stationary optical shutters, optical switches, thermos optical modulators due to phase transition characteristics of vanadium oxide<sup>[163]</sup>. The first generation conventional single and bilayer AR coatings are still appropriate in laser applications but limited in various optical elements due to reflectance minima at smaller wavelength region and AOI dependency. Multilayer AR coatings resolve this issue and are used in for the past several decades at market level, but now these are replaced by more advanced AR coatings due to its complex fabrication process, and economically expensive constraints its usage at a commercial level. Moth eye resembling bionic nanostructures resolves the issues of omnidirectional AR and replaces previous coatings in different optic equipment for enhancing transmittance due to ease of fabrication and low cost in comparison with multilayer coating stack. These moth eye and inverse moth eye nanostructures are fabricated in anechoic chambers to reduce microwave reflections in millimetres<sup>[164-166]</sup>. Similarly, moth eye nanostructures deposit on organic solar cell improves cell performance. Nowadays the fabrication techniques are environmentally friendly which offers researchers compatible environmental approaches for technological innovation in optics fields. AR coatings are widely used in photovoltaics application, but still, there is an issue of their mechanical resilience and strong adhesion strength. About their performance in outdoor applications, and environmental exposure to a long time, causes the AR coating to peel off from substrate material or the coating undergoes scratches debonding, sometimes AR coatings faces the thermal resistivity issues. Ceramic AR coatings undergo brittle fracture due

to micro cracks generation and voids present in comparison with polymer AR nanocomposites which undergoes ductile failure and less damage [166]. It is an important area to improve the mechanical strength of AR coatings for its harsh environmental exposure. Sometimes humidity or thermal coefficients difference influence the AR coating properties and the coating undergoes delamination and peel off at the interfacial area. Thermal stability is also an important parameter which cannot be neglected before designing an AR coating. HfO<sub>2</sub> bilayer AR coatings are thermally stable up to 300°C with tunability applicable in Laser induced damage threshold applications [44]. Researchers should focus their attention towards the polymer AR materials which undergo ductile failure with consistent performance and mechanical durability for a long duration. Compressive and tensile failure of AR coating should also be considered during AR fabrication and design because when a low thermal expansion coating is deposited on a substrate having high thermal coefficient than AR coating undergoes compressional failure and it bends inside during heat exposure. In opposite case, the coating expands and influence overall AR efficiency and mechanical stability. The thermal coefficient of AR coating and substrate is also necessary to maintain the mechanical stability of coating before fabrication. Wetting and non-wetting properties of an AR coating enhance its functionality in diverse fields. Non-wetting AR coatings play an influential role in self-cleaning ability. Hydrophilic AR coatings have potential application in underwater applications such as binoculars or submarines windows. In future researchers must focus on hybrid multifunctional efficient AR coatings keeping their mechanical durability in affordable and economical expenses. New technological development in optoelectronic devices enhances the AR efficiency and product improvisation. The predominated biological natural features give innovation to fabricate efficient, sophisticated AR coating in different species such as squids eyes or butterflies gyroids but it is a challenge to overcome the fragile nanostructures for their practical applicability at commercial scale. Optical simulations are essential in designing AR coatings and tailoring the properties according to application demand. In optics field, a lot of multifunctional AR coatings have been reported earlier, but it is worthwhile to design a single coating with additional properties. The long term mechanical stability, thermal stability, with a low-cost fabrication process, thin coating, superamphiphobic property, scratch resistivity and AR omnidirectional efficiency over a broad range of the spectrum with antiglare property is still a challenge to bring the lab prepare AR coatings in real applications. In one word multifunctional hybrid AR coating is still technically thought-provoking and needs to advance and a challenge for future researchers.

## ACKNOWLEDGEMENT

The authors are grateful to the financial support by the National Basic Research Program of China (973 program, Grant No. 2013CB934301), the National Natural Science Foundation of China (Grant No. 51531006 and No. 51572148), the Research Project of Chinese Ministry of Education (Grant No. 113007A), and the Tsinghua University Initiative Scientific Research Program.

## REFERENCES

1. Khan SB, et al. Nanorod Array as High-Performance and High-Temperature Antireflective Coating. *Adv Mater Interf* 2017;4:1600892.
2. Volpian OD, et al. Magnetron discharge sputtering for fabrication of nanogradient optical coatings. *J Phys: Conf Ser* 2015;652:012009.
3. Kisiel A, et al. The influence of a light beam on the electroreflectance spectra of Germanium. *Phys Status Solidi* 1977;83:35-39.
4. Harman PM. *Through the Looking-Glass and What Maxwell Found There*: Springer Netherlands 1995;79-93
5. Query MR. Direct Solution of the Generalized Fresnel Reflectance Equations. *J Opt Soc Am* 1969;36:1101-1107.
6. Lim J, et al. Fabrication of an Antireflective Nanodome Array with High Packing Density for Photovoltaic Applications. *J Nanomater* 2015;2015:1-6.
7. Han J, et al. Antireflection/antifogging coatings based on nanoporous films derived from layered double hydroxide. *Chem Eng J* 2011;169:371-378.
8. Tan T, et al. Structure and optical properties of HfO<sub>2</sub> thin films on silicon after rapid thermal annealing. *Opt Mater* 2010;32:432-435.
9. Garshin AP and Aiko-Shvaikovskii VE. Theoretical analysis of defect formation processes in silicon nitride. *Refract Ind Ceram* 1998;39:169-176.
10. Krokhnin A. *Effective medium theory*. International 2014.
11. Menegotto T and Horowitz F. Anisotropic effective medium properties from interacting Ag nanoparticles in silicon dioxide. *Appl Opt* 2014;53:2853-2859.

12. Choy TC. Effective medium theory : principles and applications. Oxford University Press 2015.
13. Groep JVD, et al. Single-Step Soft-Imprinted Large-Area Nanopatterned Antireflection Coating. *Nano Lett* 2015;15:4223.
14. Floch HG and Belleville PF. A scratch-resistant single-layer antireflective coating by a low temperature sol-gel route. *J Sol-Gel Sci Technol* 1994;1:293-304.
15. Zhang X, et al. Self-Cleaning Particle Coating with Antireflection Properties. *Chem of Mater* 2005;17.
16. Hensch G and Deubener J. Compatibility of antireflective coatings on glass for solar applications with photocatalytic properties. *Solar Energy* 2012;86:831-836.
17. Xu L, et al. Fabrication of visible/near-IR antireflective and superhydrophobic coatings from hydrophobically modified hollow silica nanoparticles and poly(methyl methacrylate). *Rsc Adv* 2012;2:12764-12769.
18. Hedayati MK, et al. Photo-driven Super Absorber as an Active Metamaterial with a Tunable Molecular-Plasmonic Coupling. *Adv Opt Mater* 2015;2:705-710.
19. Moghal J, et al. High-performance, single-layer antireflective optical coatings comprising mesoporous silica nanoparticles. *Acs Appl Mater Interf* 2012;4:854-859.
20. Zheng L, et al. Hierarchically ordered arrays based on solvent vapor annealed colloidal monolayers for antireflective coating. *Thin Solid Films* 2013;544:403-406.
21. Krasilnik ZF, et al. Erbium Doped Silicon Single- and Multilayer Structures for LED and Laser Applications. *Mrs Proceedings* 2005;866.
22. Fu Y. Light Emission and Slot Waveguide Effect in erbium-doped silicon dioxide/silicon nanocrystalline Multilayer Structures. *Dissertations & Theses - Gradworks*. 2012.
23. Martin AS, et al. A few-monolayer organic photodiode. *Adv Func Mater* 2010;7:45-50.
24. Smet PF, et al. Selecting Conversion Phosphors for White Light-Emitting Diodes. *J Electrochem Soc* 2011;158:R37-R54.
25. Du K, et al. The rate equation based optical model for phosphor-converted white light-emitting diodes. *J Phys D Appl Phys* 2017;50.
26. Ye L, et al. Mechanically stable single-layer mesoporous silica antireflective coating on solar glass. *Rsc Adv* 2014;4:35818-35822.
27. Glaubitt W and Lobmann P. Antireflective coatings prepared by sol-gel processing: Principles and applications. *J Eur Ceram Soc* 2012;32:2995-2999.
28. Bouhafs D, et al. Design and simulation of antireflection coating systems for optoelectronic devices: Application to silicon solar cells. *Solar Energy Mater Solar Cells* 1998;52:79-93.
29. Abdul Hadi S, et al. Design Optimization of Single-Layer Antireflective Coating for GaAs P /Si Tandem Cells With , 0.17, 0.29, and 0.37. *Photovoltaics IEEE J* 2014;5:425-431.
30. Kern W and Tracy E. Titanium dioxide antireflection coating for silicon solar cells by spray deposition. *RCA Rev; (United States)* 1980;41:133-180.
31. Raut HK, et al. Porous SiO<sub>2</sub> anti-reflective coatings on large-area substrates by electrospinning and their application to solar modules. *Solar Energy Mater Solar Cells* 2013;111:9-15.
32. Lee SE, et al. Double-layer anti-reflection coating using MgF<sub>2</sub> and CeO<sub>2</sub> films on a crystalline silicon substrate. *Thin Solid Films* 2000;376:208-213.
33. Chen D, et al. Development of Anti-Reflection (AR) Coating on Plastic Panels for Display Applications. *J Sol-Gel Sci Technol* 2000;19:77-82.
34. Wright DN, et al. Double layer anti-reflective coatings for silicon solar cells. *IEEE* 2005;1237-1240.
35. Dhungel SK. Double Layer Antireflection Coating of MgF<sub>2</sub>/SiNx for Crystalline Silicon Solar Cells. *J Phys Soc* 2006;49:885-889.
36. Zhang X, et al. Double-layered TiO<sub>2</sub>-SiO<sub>2</sub> nanostructured films with self-cleaning and antireflective properties. *J Phys Chem B* 2006;110:25142-25148.

37. Zhang H, et al. Antireflective and Self-cleaning Properties of SiO<sub>2</sub>/TiO<sub>2</sub> Double-Layer Films Prepared by Cost-Effective Sol-Gel Process 2015;28:777-780.
38. Jin B, et al. Rational Design and Construction of Well-Organized Macro-Mesoporous SiO<sub>2</sub>/TiO<sub>2</sub> Nanostructure toward Robust High-Performance Self-Cleaning Antireflective Thin Films. *Acs Appl Mater Interf* 2017;9.
39. Xiao B, et al. Sol-gel preparation of double-layer tri-wavelength antireflective coating. *J Sol-Gel Sci Technol* 2012;64:276-281.
40. Bao L, et al. Hollow Rodlike MgF<sub>2</sub> with an Ultralow Refractive Index for the Preparation of Multifunctional Antireflective Coatings. *Langmuir* 2017.
41. De S, et al. Wavelength Selective Antireflective Coatings on Plastics with Hydrophobic Surfaces. *Ind Eng Chem Res* 2013;52:7737-7745.
42. Zhang XX, et al. Template-Free Sol-Gel Preparation of Superhydrophobic ORMOSIL Films for Double-Wavelength Broadband Antireflective Coatings. *Adv Func Mater* 2013;23:4361-4365.
43. Khan SB, et al. Antireflective coatings with enhanced adhesion strength. *Nanoscale* 2017.
44. Khan SB, et al. Antireflective Coatings: HfO<sub>2</sub> Nanorod Array as High-Performance and High-Temperature Antireflective Coating. *Adv Mater Interf* 2017;4:1600892.
45. Aroutiounian VM, et al. Almost zero reflectance of a silicon oxynitride/porous silicon double layer antireflection coating for silicon photovoltaic cells. *J Phys D Appl Phys* 2006;39:1623.
46. Kamura H, et al. plastic lens comprising multilayer antireflective film and method for manufacturing same. US; 2009.
47. Zhu JQ, et al. Multilayer antireflective and protective coatings comprising amorphous diamond and amorphous hydrogenated germanium carbide for ZnS optical elements. *Thin Solid Films* 2008;516:3117-22.
48. Chao-Quan HU, et al. Preparation and Properties for Germanium Carbide Double-Layer Films Used as Antireflection and Protection Coatings. *Chinese J Liquid Cryst Displays* 2010;25:339-341.
49. Jeong O, et al. Broadband Plasma-Sprayed Anti-reflection Coating for Millimeter-Wave Astrophysics Experiments. *J Low Temp Phys* 2016;184:1-6.
50. Matsumura T, et al. Millimeter-wave broadband antireflection coatings using laser ablation of subwavelength structures. *Appl Opt* 2016;55:3502.
51. Mazur M, et al. Functional photocatalytically active and scratch resistant antireflective coating based on TiO<sub>2</sub> and SiO<sub>2</sub>. *Appl Surf Sci* 2016;380:165-171.
52. Mazur M, et al. TiO<sub>2</sub> /SiO<sub>2</sub> multilayer as an antireflective and protective coating deposited by microwave assisted magnetron sputtering. *Opto-Electron Rev* 2013;21:233-238.
53. Wang KX, et al. Condition for perfect antireflection by optical resonance at material interface. *Optica* 2014;1:388.
54. Spinelli P, et al. Optical Impedance Matching Using Coupled Plasmonic Nanoparticle Arrays. *Nano Lett* 2011;11:1760.
55. Li X, et al. Porous Polymer Films with Gradient-Refractive-Index Structure for Broadband and Omnidirectional Antireflection Coatings. *Adv Funct Mater* 2010;20:259-265.
56. Lien SY, et al. Tri-layer antireflection coatings (SiO<sub>2</sub>/SiO<sub>2</sub> -TiO<sub>2S</sub>/TiO<sub>2</sub> ) for silicon solar cells using a sol-gel technique. *Solar Energy Mater Solar Cells* 2006;90:2710-2719.
57. Chen CC, et al. Preparation of organic-inorganic nano-composites for antireflection coatings. *J Non-Crystal Solid* 2008;354:3828-3835.
58. Belleville PF. Optical thin films from the sol-gel process. *Opt Interference Coatings* 1994;2253.
59. Sabnis RW, et al. Organic polymeric antireflective coatings deposited by chemical vapor deposition. US; 2005.
60. Druzhinin A, et al. Si nanowires for antireflective coatings of photovoltaic cells. *Int Conf Modern Probl Radio Eng Telecommun Comput Sci* 2012;484-485.
61. Chen HL, et al. Reduction of substrate alkaline contamination by utilizing multi-layer bottom antireflective coating structures in ArF lithography. *Microprocesses and Nanotechnol Conference 2001 International* 2002;230-231.
62. Gil-Rostra J, et al. Tuning the transmittance and the electrochromic behavior of Co<sub>x</sub>Si<sub>y</sub>O<sub>z</sub> thin films prepared by magnetron sputtering at glancing angle. *Solar Energy Mater Solar Cells* 2014;123:130-138.

63. Winderbaum S, et al. Application of plasma enhanced chemical vapor deposition silicon nitride as a double layer antireflection coating and passivation layer for polysilicon solar cells. *J Vacuum Sci Technol A Vacuum Surf Films* 1997;15:1020-1025.
64. Zhao J, et al. Twenty-four percent efficient silicon solar cells with double layer antireflection coatings and reduced resistance loss. *Appl Phys Lett* 1995;66:3636-3638.
65. Jamali H, et al. Evaluation of chemical and structural properties of germanium-carbon coatings deposited by plasma enhanced chemical vapor deposition. *J Alloys Comp* 2015;646:360-367.
66. Hosoda Y, et al. Physical Vapor Deposition of Fluoropolymer Thin Films and Their Characteristics as Antireflective Coating. *Tech Report of Ieice Ome* 2009;109:3-7.
67. Melninkaitis A, et al. Optical characterization of antireflective sol-gel coatings fabricated using dip coating method. *Proc SPIE – Int Soc for Opt Eng* 2006;6403.
68. Tortai JH. Modeling of ultrathin resist film structure after spin-coating and post-application bake: Elsevier Sci Ltd 2004.
69. Norrman K, et al. Studies of spin-coated polymer films. *Ann Rep Sect "C" (Physical Chem)* 2005;101:174-201.
70. Ogi T, et al. Fabrication of a large area monolayer of silica particles on a sapphire substrate by a spin coating method. *Colloids Surf A Physicochem Eng Aspects* 2007;297:71-78.
71. Biswas PK, et al. Porous anti-reflective silica coatings with a high spectral coverage by sol-gel spin coating technique. *J Mater Sci Lett* 2003;22:181-183.
72. Wang Y, et al. Spherical antireflection coatings by large-area convective assembly of monolayer silica microspheres. *Solar Energy Mater Solar Cells* 2009;93:85-91.
73. Hiller JA, et al. Reversibly erasable nanoporous anti-reflection coatings from polyelectrolyte multilayers. *Nature Mater* 2002;1:59.
74. Chen HL, Chuang SY, Lin CH, Lin YH. Using colloidal lithography to fabricate and optimize sub-wavelength pyramidal and honeycomb structures in solar cells. *Opt Express* 2007;15:14793.
75. Antony S, et al. A Comparison between the Optical Properties of Amorphous and Crystalline Monolayers of Silica Particles†. *Langmuir* 1999;15:5257-5264.
76. Zhang L, et al. Mechanically stable antireflection and antifogging coatings fabricated by the layer-by-layer deposition process and postcalcination. *Langmuir Acs J Surf Colloids* 2008;24:10851-10857.
77. Park MS and Kim JK. Broad-band antireflection coating at near-infrared wavelengths by a breath figure. *Langmuir Acs J Surf Colloids* 2005;21:11404-11408.
78. Zhang L, et al. Mechanically stable antireflection and antifogging coatings fabricated by the layer-by-layer deposition process and postcalcination. *Langmuir the Acs J Surf Colloids* 2008;24:10851-10857.
79. Park MS and Kim JK. Broad-band antireflection coating at near-infrared wavelengths by a breath figure. *Langmuir the Acs J Surf Colloids* 2005;21:11404-11408.
80. Joo W, et al. Block copolymer film with sponge-like nanoporous structure for antireflection coating. *Langmuir Acs J Surf Colloids* 2006;22:7960.
81. Walheim S, et al. Nanophase-Separated Polymer Films as High-Performance Antireflection Coatings. *Science* 1999;283:520-522.
82. Melninkaitis A, et al. Optical characterization of anti-reflective sol-gel coatings fabricated using dip coating method: *Int Soc Optics Photon* 2006.
83. Xin YE, et al. Sub-wavelength nano-porous silica anti-reflection coatings fabricated by dip coating method. *Optics Precision Eng* 2015;23:1233-1239.
84. Cathro K, et al. Silica low-reflection coatings for collector covers, by a dip-coating process. *Solar Energ* 1984;32:573-579.
85. Cao X, et al. Nanoporous thermochromic VO<sub>2</sub> (M) thin films: controlled porosity, largely enhanced luminous transmittance and solar modulating ability. *Langmuir the Acs J Surf Colloids* 2014;30:1710.
86. Salvaggio MG, et al. Functional nano-textured titania-coatings with self-cleaning and antireflective properties for photovoltaic surfaces. *Solar Energ* 2016;125:227-242.

87. Mohite KC, et al. Characterization of silicon oxynitride thin films deposited by electron beam physical vapor deposition technique. *Mater Lett* 2003;57:4170-4175.
88. Eriksson TS and Granqvist CG. Infrared optical properties of electron-beam evaporated silicon oxynitride films. *Appl Opt* 1983;22:3204.
89. Romach MM, et al. Inverted Cylindrical Magnetron Sputtering of Optical Coatings. *Soc of Vacuum Coaters Tech Conf* 2015;233-238.
90. Mazingue T, et al. Nanostructured ZnO coatings grown by pulsed laser deposition for optical gas sensing of butane. *J Appl Phys* 2005;98:349.
91. Sun XW and Kwok HS. Optical properties of epitaxially grown zinc oxide films on sapphire by pulsed laser deposition. *J Appl Phys* 1999;86:408-11.
92. Goetz B, et al. Adhesion of hydrophobic coatings on eyeglass lenses. US; 2008.
93. Beißwenger S, et al. Large-scale antireflective coatings on glass produced by reactive magnetron sputtering. *Surf Coat Technol* 1998;60:624–628.
94. Bartzsch H, et al. Graded refractive index layer systems for antireflective coatings and rugate filters deposited by reactive pulse magnetron sputtering. *Surf Coat Technol* 2004;180–181:616-620.
95. Roquiny P, et al. control of titanium nitride coatings produced by reactive magnetron sputtering at temperature less than 100°C. *Surf Coat Technol* 1999;116–119:278-283.
96. Xi JQ, et al. Very low-refractive-index optical thin films consisting of an array of SiO<sub>2</sub> nanorods. *Opt Lett* 2006;31:601-603.
97. Nam SH, et al. Growth of TiO<sub>2</sub> anti-reflection layer on textured Si (100) wafer substrate by metal-organic chemical vapor deposition method. *J Nanosci Nanotechnol* 2011;11:7315-7318.
98. Kennedy SR and Brett MJ. Porous broadband antireflection coating by glancing angle deposition. *Appl Opt* 2003;42:4573-4579.
99. Yuan H, et al. Design and fabrication of multilayer antireflection coating for optoelectronic devices by plasma enhanced chemical vapor deposition. *Acta Physica Sinica* 2010;59:7239-7244.
100. Khan SB, et al. Morphological Influence of TiO<sub>2</sub> Nanostructures (nanozigzag, nanohelics and nanorod) on Photocatalytic Degradation of organic dyes. *Appl Surf Sci* 2016;400.
101. Zhou Q, et al. A Simple Model to Describe the Rule of Glancing Angle Deposition. *Mater Trans* 2011;52:469-473.
102. Sanchezvalencia JR, et al. Growth Assisted by Glancing Angle Deposition (GAGLAD): A new technique to engineer highly porous anisotropic thin films. *Acs Appl Mater Interf* 2016;8.
103. Chen Y, et al. Sputtered TiO<sub>2</sub> Films for Photovoltaic Cell's Antireflection Coating. *Int J Nanosci* 2012;11:139
104. Chhajed S, et al. Nanostructured multilayer graded-index antireflection coating for Si solar cells with broadband and omnidirectional characteristics. *Appl Phys Lett* 2008;93:161.
105. Sun CH, et al. Broadband moth-eye antireflection coatings on silicon. *Appl Phys Lett* 2008;92:061112.
106. Min WL, et al. Bioinspired broadband antireflection coatings on GaSb. *Appl Phys Lett* 2008;92:689.
107. Gwon HJ, et al. Superhydrophobic and Antireflective Properties of the Hierarchically Nanotextured Glass Surfaces. *Sci Adv Mater* 2015;7:695.
108. Wang Y, et al. Biomimetic corrugated silicon nanocone arrays for self-cleaning antireflection coatings. *Nano Res* 2010;3:520-527.
109. Chen JY, et al. Biomimetic nanostructured antireflection coating and its application on crystalline silicon solar cells. *Opt Express* 2011;19:14411-14419.
110. Prasad A, et al. Porous silicon oxide anti-reflection coating for solar cells. *J Electrochem Soc* 1982;129:596-599.
111. Schirone L, et al. Chemically etched porous silicon as an anti-reflection coating for high efficiency solar cells. *Thin Solid Films* 1997;297:296-298.
112. Fujii H, et al. Formation and application of porous silicon. *Mater Sci Eng R* 2002;39:93-141.



113. Williams FE and Nicoll FH Properties of Low Reflection Films Produced by the Action of Hydrofluoric Acid Vapor. *Josa* 1943.
114. Taylor HD, et al. Chemical methods for increasing the transparency of glass surfaces. *J Opt Soc Am* 1941;31:34-38.
115. Clapham, et al. Reduction of Lens Reflexion by the "Moth Eye" Principle. *Nature* 1973;244:281-282.
116. Leem JW, et al. Broadband and omnidirectional highly-transparent coverglasses coated with biomimetic moth-eye nanopatterned polymer films for solar photovoltaic system applications. *Solar Energy Mater Solar Cells* 2015;134:45-53.
117. Park SC, et al. Fabrication and characterization of moth-eye mimicking nanostructured convex lens. *Microelectronic Eng* 2016;158:35-40.
118. Lee HK, et al. Improved device performance of AlGaInP-based vertical light-emitting diodes with low-n ATO antireflective coating layer. *Microelectronic Eng* 2013;104:29-32.
119. Kleptsyn V. Reflective color filter and color display device 2016.
120. Guldin S and Steiner U. Coating e.g. self-cleaning antireflective coating for solar panel, electroluminescent device, spectacle, telescope and microscope, comprises mesoporous inorganic skeleton having photocatalytic particles, and has specified porosity. *Acta Chemica Scandinavica* 1978;32:943-955.
121. Assadi MK and Hanaei H. Transparent Carbon Nanotubes (CNTs) as Antireflection and Self-cleaning Solar Cell Coating: Springer International Publishing; 2017.
122. Kondo T, et al. Enhancement of light extraction efficiency of blue-light-emitting diodes by moth-eye structure. *OPTO* 2010; 76021M-M-7.
123. Yan X, et al. Deep-ultraviolet tailored- and low-refractive index antireflection coatings for light-extraction enhancement of light emitting diodes. *J Appl Phys.* 2013;113:172-7.
124. Pauchard A, et al. A silicon blue/UV selective stripe-shaped photodiode. *Sensor Actuators A Phys* 1999;76:172-177.
125. Morita D, et al. Over 200 mW on 365 nm ultraviolet light emitting diode of GaN-free structure. *Physica Status Solidi* 2010;200:114-117.
126. Chin AK, et al. Al<sub>2</sub>O<sub>3</sub> as an antireflection coating for InP/InGaAsP LEDs. *J Vacuum Sci Technol B Microelectron Nanometer Struct* 1983;1:72-73.
127. Weaver M, Takashima Y. LED optical lens. WO 2012.
128. Liu C, et al. Improvement of OLED properties with anti-reflection coatings. *Soc Photo-Opt Instrument Eng* 2010.
129. Chou YH, et al. AZO films with Al nano-particles to improve the light extraction efficiency of GaN-based light-emitting diodes. *Integr Optoelectronic Devices* 2008;68941C-C-6.
130. Chen Zhanxu, et al. Enhancing light extraction of GaN-based blue light-emitting diodes by a tuned nanopillar array. *Chinese Phys B: Eng* 2014;23:500-504.
131. Yoo H, et al. Enhanced light extraction efficiency of GaN-based LED fabricated by multi-chip array. *Opt Mater Express* 2015;5:1098-1108.
132. Park J, et al. Enhancement of light extraction in GaN-based light-emitting diodes by Al<sub>2</sub>O<sub>3</sub> -coated ZnO nanorod arrays. *J Alloys Comp* 2014;611:157-160.
133. Kim KK, et al. Enhanced light extraction efficiency of GaN-based light-emitting diodes with ZnO nanorod arrays grown using aqueous solution. *Appl Phys Lett* 2009;94:103502.
134. An SJ, et al. Enhanced light output of GaN-based light-emitting diodes with ZnO nanorod arrays. *Appl Phys Lett* 2008;92:1274.
135. Choi PJ, et al. Light extraction enhancement of GaN based light emitting diodes by ZnO nanorod arrays. *J Nanosci Nanotechnol* 2014;14:5965-5969.
136. Chiu CH, et al. Oblique electron-beam evaporation of distinctive indium-tin-oxide nanorods for enhanced light extraction from InGaN/GaN light emitting diodes. *Opt Express* 2009;17:21250-256.
137. Kato K, et al. Changes in electrical and structural properties of indium oxide thin films through post-deposition annealing. *Thin Solid Films* 2011;520:110-116.

- 138.Heo SB, et al. Effect of Post-Deposition Annealing on the Structural, Optical and Electrical Properties of Ti-doped Indium Oxide. *Thin Films* 2016;54:775-779.
- 139.Pham DP, et al. Influence of addition of indium and of post-annealing on structural, electrical and optical properties of gallium-doped zinc oxide thin films deposited by direct-current magnetron sputtering. *Thin Solid Films* 2015;583:201-204.
- 140.Vicente GS, Bayyn R, Germ6n N, Morales A. Long-term durability of sol–gel porous coatings for solar glass covers. *Thin Solid Films* 2009;517:3157-3160.
- 141.Deubener J, et al. Glasses for solar energy conversion systems. *J Eur Ceram Soc* 2009;29:1203-1210.
- 142.S6nchez-Friera P, et al. Analysis of degradation mechanisms of crystalline silicon PV modules after 12 years of operation in Southern Europe. *Progr Photovoltaics Res Appl* 2011;19:658–666.
- 143.Li J, et al. Design, preparation, and durability of TiO<sub>2</sub> /SiO<sub>2</sub> and ZrO<sub>2</sub> /SiO<sub>2</sub> double-layer antireflective coatings in crystalline silicon solar modules. *Solar Energ* 2013;89:134-142.
- 144.Onishi Y, et al. Application of polysilanes for deep-UV antireflective coating. *Microlithography*1999.
- 145.Hanaei H, et al. Highly efficient antireflective and self-cleaning coatings that incorporate carbon nanotubes (CNTs) into solar cells: A review. *Renew Sust Energ Rev* 2016;59:620-635.
- 146.Lu F, et al. An improved polymer solar cell incorporating single-wall carbon nanotubes. *J Modern Optics* 2014;61:1761-1766.
- 147.Lee J, et al. Polymer Quantum Dot-Sensitized Solar Cell Incorporating Single-Walled Carbon Nanotubes. *J Nanosci Nanotechnol* 2017;17:5496-500.
- 148.Huang YC, et al. High-performance ITO-free spray-processed polymer solar cells with incorporating ink-jet printed grid. *Org Electron* 2013;14:2809-2817.
- 149.Li Z, et al. Enhancement of the power conversion efficiency of polymer solar cells by incorporating PbSe quantum dots. *J Mater Sci* 2015;50:840-847.
- 150.Derbalhabak H, et al. Functionalized single wall carbon nanotubes improve the properties of polymer solar cells. *Proc SPIE - The Int Soc Opt Eng* 2010;7750.
- 151.Sumit Chaudhary, et al. Hierarchical Placement and Associated Optoelectronic Impact of Carbon Nanotubes in Polymer-Fullerene Solar Cells. *Nano Lett* 2007;7:1973.
- 152.Chang MY, et al. Polymer solar cells incorporating one-dimensional polyaniline nanotubes. *Org Electron* 2008;9:1136-1139.
- 153.Osterwald CR and McMahan TJ. History of accelerated and qualification testing of terrestrial photovoltaic modules: A literature review. *Progr Photovoltaics Res Appl* 2009;17:11-33.
- 154.Tong HS, et al. Multilayer antistatic/antireflective coating for display device. US 5652477 A; 1997.
- 155.Hu CM, et al. Multilayer antireflective coating for video display panel. US 5523649 A; 1996.
- 156.Bright CI, et al. Multi-component films for optical display filters. US 20090109537 A1;2014.
- 157.Okamura T, et al. Optical filters for plasma display panels using organic dyes and sputtered multilayer coatings. *J Sci Technol A Vacuum Surf Films* 2001;19:1090-1094.
- 158.Okamura T, et al. Optical filters for plasma-display panels using organic dyes and conductive mesh layers by using a roll-to-roll etching process. *J Soc for Inf Display* 2012;12:527-531.
- 159.Boudot M. Design and characterization of an innovative sol gel antireflective coating for embedded system screens in aeronautic. 2014.
- 160.Keshavarz HM and Elbahri M. Antireflective Coatings: Conventional Stacking Layers and Ultrathin Plasmonic Metasurfaces, *A Mini-Rev Mater* 2016;9:497.
- 161.Lin CL, et al. Electrochromic and photoelectrochromic properties of sol–gel derived tungsten trioxide/titania composite thin films. *Res Chem Intermediates* 2016:1-10.
- 162.Soltani M, et al. Thermochromic vanadium dioxide (VO<sub>2</sub>) smart coatings for switching applications. *Appl Phys in the 21st Century* 2008;1-23.
- 163.Harris DC. Materials for Infrared Windows and Domes: Properties and Performance. *Opt Photon News* 2001;12:54.

164. Mirotznik MS, et al. Broadband Antireflective Properties of Inverse Motheye Surfaces. *IEEE Transactions on Antennas Propagation* 2010;58:2969-2680.
165. Osbond P. Plasma sprayed anti-reflection coatings for microwave optical components. *Adv Mater* 1992;4:807-809.
166. Druffel T, et al. Mechanical comparison of a polymer nanocomposite to a ceramic thin-film anti-reflective filter. *Nanotechnology* 2006;17:3584-3590.